Macromolecules

Article

Impact of Imidazolium-Based Ionic Liquids on the Curing Kinetics and Physicochemical Properties of Nascent Epoxy Resins

Andrzej Dzienia,* Magdalena Tarnacka, Kajetan Koperwas, Paulina Maksym, Andrzej Zięba, Joanna Feder-Kubis, Kamil Kamiński,* and Marian Paluch

Read Online

ACCESS | Metrics & More | Article Recommendations | Supporting Information

ABSTRACT: We investigated the influence of anion type (salicylate, $[(MOB)MIm][Sal]$, vs chloride, $[(MOB)MIm][Cl]$) of imidazolium-based ionic liquid (IL) and its content on the curing kinetics of bisphenol A diglicydyl ether (DGEBA of molecular weight M_n = 340 g/mol). Further physicochemical properties (i.e., glass transition temperature, T_g, and conductivity, σ_{dc}) of produced polymers were investigated. The polymerization of the studied systems was examined at various molar ratios (1:1, 10:1, and 20:1) at different reaction temperatures ($T_{reaction}$ = 353−383 K) by using differential scanning calorimetry (DSC).

Interestingly, both DGEBA/IL compositions studied herein revealed significantly different reaction kinetics and yielded materials of completely distinct physical properties. Surprisingly, in contrast to $[(MOB)MIm][Cl]$, for the low concentration of $[(MOB)MIm][Sal]$ in the reaction mixture, an additional step in the kinetic curves, likely due to the combined enhanced initiation activity of anion (salicylate)−cation (imidazolium-based), was noted. To thoroughly analyze the kinetics of all studied systems, including the two-step kinetics of DGEBA/$[(MOB)MIm][Sal]$, we applied a new approach that relies on the combination of the two phenomenological Avrami equations. Analysis of the determined constant rates revealed that the reaction occurring in the presence of the salicylate anion is characterized by higher activation energy with respect to those with the chloride. Moreover, DGEBA/$[(MOB)MIm][Sal]$ cured materials have higher T_g in comparison to DGEBA polymerized with $[(MOB)MIm][Cl]$ independent of the IL concentration. This fact might indicate that, most likely, the products of hardening are highly cross-linked (high T_g) or oligomeric linear polymers (low T_g) in the former and latter cases, respectively. Such a change in the chemical structure of the polymer is also reflected in the dc conductivity measured at the glass transition temperature, which is much higher for DGEBA cured with $[(MOB)MIm][Cl]$. Herein, we have clearly demonstrated that the type of anion has a crucial impact on the polymerization mechanism, kinetics, and properties of produced materials.
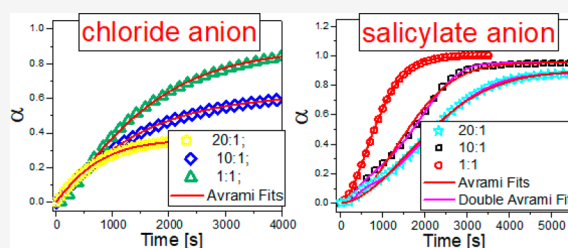
1. INTRODUCTION

Epoxy resins, due to their versatility, are one of the most important groups of thermosetting macromolecules. They are widely used, for example, in the marine and aerospace industry and allow to construct and develop electronic devices, coatings, paints, or adhesives.[1−4] Such an impressive number of applications is caused by the fact that the final properties of these materials can be easily tuned by either optimization of the system composition or the curing protocol (choice of pressure, temperature, heating rate, or variation in the external parameters such as light irradiation and sonification).[5−12] Consequently, solid-state polymers with well-defined mechanical characteristics, degree of cure, cross-linking density, glass transition temperature, adhesivity, thermal stability, moisture, corrosion, fungal, electric, and chemical resistance can be synthesized.[13−15]

Recently, a great effort has been made to obtain high-performance materials that link excellent thermomechanical properties with unique features like self-healing, shape memory, or high (superprotonic) conductivity.[16−22] In

particular, the last feature (conductivity) has attracted increasing attention since highly conductive materials can be used in the low- and intermediate-temperature fuel cell applications, reducing environmental pollution such as CO_2 emission.[23−25] To produce systems of enhanced conductivity, different strategies are adopted. Briefly, one can mention the synthesis of (i) conjugated polymers with unsaturated bonds such as poly(acetylene), poly(pyrrole), poly(thiophene), and poly(3,4-ethylenedioxythiophene),[26,27] (ii) poly(ionic liquid)s (PILs),[28,29] and (iii) composites consisting of, for example, doped or ionic liquid-based epoxy resins.[22,30,31] Although all of the mentioned classes of polymers have many desired properties and benefits, it seems that because of its excellent
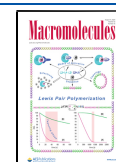
versatility and general performance, the last group of materials seems to be extremely important and interesting.[20,30−33]

It is well-known that epoxy-based conductive materials can be obtained via two different approaches: either direct polymerization with the ionic liquids (ILs) acting as monomers and/or hardening agents[32,33] or the postmodification of produced classical nonconducting epoxy resins with different fillers (i.e., carbon fibers or nanotubes,[20,21,34] graphene, metallic fillers, CPs, or nonreactive ILs).[20,21,34] Consequently, we can obtain various conducting materials (polymers or composites) containing the ionic moieties (anions and cations) within the polymer network and therefore enforcing the different charge transport.[32,33,35−37]

Herein, we investigated the influence of anion type (salicylate vs chloride) of imidazolium-based IL as well as its content on the curing kinetics and physicochemical properties (i.e., glass transition temperature, T_g, and conductivity, σ_{dc}) of a hardened bisphenol A diglicydyl ether (DGEBA of molecular weight M_n = 340 g/mol). For that purpose, two systems composed of DGEBA and [(MOB)MIm][Sal] (polymerizing system I, PS I) or [(MOB)MIm][Cl] (polymerizing system II, PS II) mixed at various molar ratios (1:1, 10:1, and 20:1) were prepared (see Scheme 1). The studied epoxy-based systems

Scheme 1. Chemical Structures of the Examined Compounds: (left) [(MOB)MIm][Sal], (middle) Epoxy Resin−DGEBA, and (right) [(MOB)MIm][Cl]

Polymerization System I - PS I
DGEBA + [(MOB)MIm][Sal]

Polymerization System II - PS II
DGEBA + [(MOB)MIm][Cl]
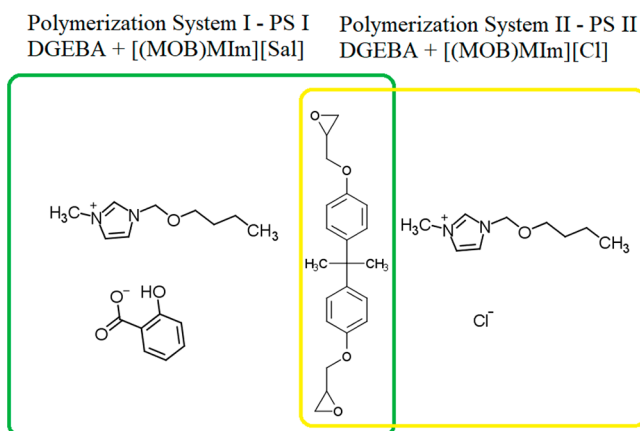
were measured (polymerized) at isothermal conditions at different reaction temperatures ($T_{reaction}$ = 353−383 K) by using differential scanning calorimetry (DSC), which provides easy and direct insight into the reaction kinetics, including the estimation of constant rates and activation energy.[38−40] Interestingly, as observed, the curing processes of DGEBA/IL systems revealed significant differences in the reaction mechanism and thermoconducting properties of newly produced materials.

2. EXPERIMENTAL SECTION

2.1. Materials. Bisphenol A diglycidyl ether (known as DGEBA of molecular weight M_n = 340 g/mol) of purity higher than 99% was supplied by Sigma-Aldrich. 1-Methylimidazole (99%), sodium salicylate (≥99.5%), paraformaldehyde (powder, 95%), hydrochloric acid (35−38%), and sulfuric acid (≥96%) were supplied by Merck, while 1-butanol (≥99%) was delivered by Alfa Aesar. The drying agents, i.e., sodium sulfate (anhydrous, pure) and phosphorus pentoxide (powder, anhydrous, ≥98%), were provided by P.O.Ch

(Gliwice, Poland). The ILs synthesis procedure is available in the Supporting Information.

The epoxy resin and curing agent were mixed with 1:1, 10:1, and 20:1 molar ratios. For example, at the 10:1 molar ratio, we used 5 g of DGEBA with 0.45 or 0.3 g of 1-butoxymethyl-1-methylimidazolium salicylate [(MOB)MIm][Sal] and 1-butoxymethyl-1-methyl-imidazolium chloride [(MOB)MIm][Cl], respectively (see Scheme 1). All samples were identically prepared in a glovebox. Immediately after preparation, they were measured by using broadband dielectric spectroscopy (BDS) and differential scanning calorimetry (DSC) techniques. All reagents were purified and then dried through the use of commonly known procedures. The same experimental protocols were applied to [(MOB)N$_{111}$][Sal] and [(MOB)N$_{111}$][Cl] (see Figure S3 in the Supporting Information).

2.2. Methods. *Differential Scanning Calorimetry (DSC).* All the DGEBA/ILs mixtures were prepared as a 1:1, 10:1, and 20:1 molar mixtures by weighed and mixed manually with the use of spatula. DSC measurements were conducted at atmospheric pressure using a Mettler-Toledo DSC apparatus. This DSC is equipped with a liquid nitrogen cooling accessory and an HSS8 ceramic sensor (heat flux sensor with 120 thermocouples). Temperature and enthalpy calibrations were performed by using indium and zinc standards. The sample was prepared in an open aluminum crucible (40 μL) outside the DSC apparatus. Each experiment was performed at isothermal conditions at $T_{reaction}$ = 353−383 K, which was followed by nonisothermal measurements. The dynamic scans were performed in the temperature range T = 233−423 K with a constant heating rate of 10 K/min. Each measurement at a given temperature was repeated three times. For each experiment, a new sample was prepared. Additionally, to determine the thermal decomposition of studied imidazolium-based ionic liquids, the samples were heated to T = 573 K with a constant heating rate of 10 K/min. Obtained DSC thermograms are presented in Figure S1.

Broadband Dielectric Spectroscopy (BDS). Dielectric permittivity $\varepsilon^*(\omega) = \varepsilon'(\omega) - i\varepsilon''(\omega)$ values at ambient pressure were measured by using the impedance analyzer (Novocontrol Alpha) over a frequency range from 1×10^{-1} to 3×10^6 Hz. The temperature was controlled by a Quatro Cryosystem using a nitrogen gas cryostat, with stability better than 0.1 K. Epoxy resin was mixed with ionic liquid at 1:1 and 10:1 molar ratio and transferred to the top of the lower plate of the capacitor. After 1 h curing at 373 K and 5 min postcuring at 423 K, a hardened system was covered with the second (upper) plate. Dielectric measurements were performed at the T_g determined from the DSC method were. The samples were placed between two stainless-steel electrodes (diameter: 20 mm; gap: 0.14 mm) and mounted inside a cryostat.

3. RESULTS AND DISCUSSION

The raw DSC data obtained upon the isothermal DSC experiments performed at the following temperatures, $T_{reaction}$ = 353−383 K, are presented in Figure 1. For the PS I system ([DGEBA]$_0$/[(MOB)MIm][Sal]$_0$ = 1:1), a significant exothermic peak related to the formation of new covalent bonds between substrates, shifting toward shorter times with an increase in temperature, is observed in all cases (see Figure 1a). A similar situation was previously noted for the other systems.[41] However, surprisingly, with a reducing concentration of [(MOB)MIm][Sal] in the curing mixture, one can note the presence of the two well-resolved peaks in the measured thermograms, most likely indicating the occurrence of an additional reaction step (Figure 1c). This effect was not detected for the 1:1 molar ratio mixture. Note that the same (two-peak) scenario can also be observed for [DGEBA]$_0$/[(MOB)MIm][Sal]$_0$ = 20:1 (see Figure S2). On the other hand, for the PS II system (DGEBA/[(MOB)MIm][Cl]), a monomodal exothermic peak, whose maximum routinely shifts to the shorter times with increasing $T_{reaction}$, can be seen
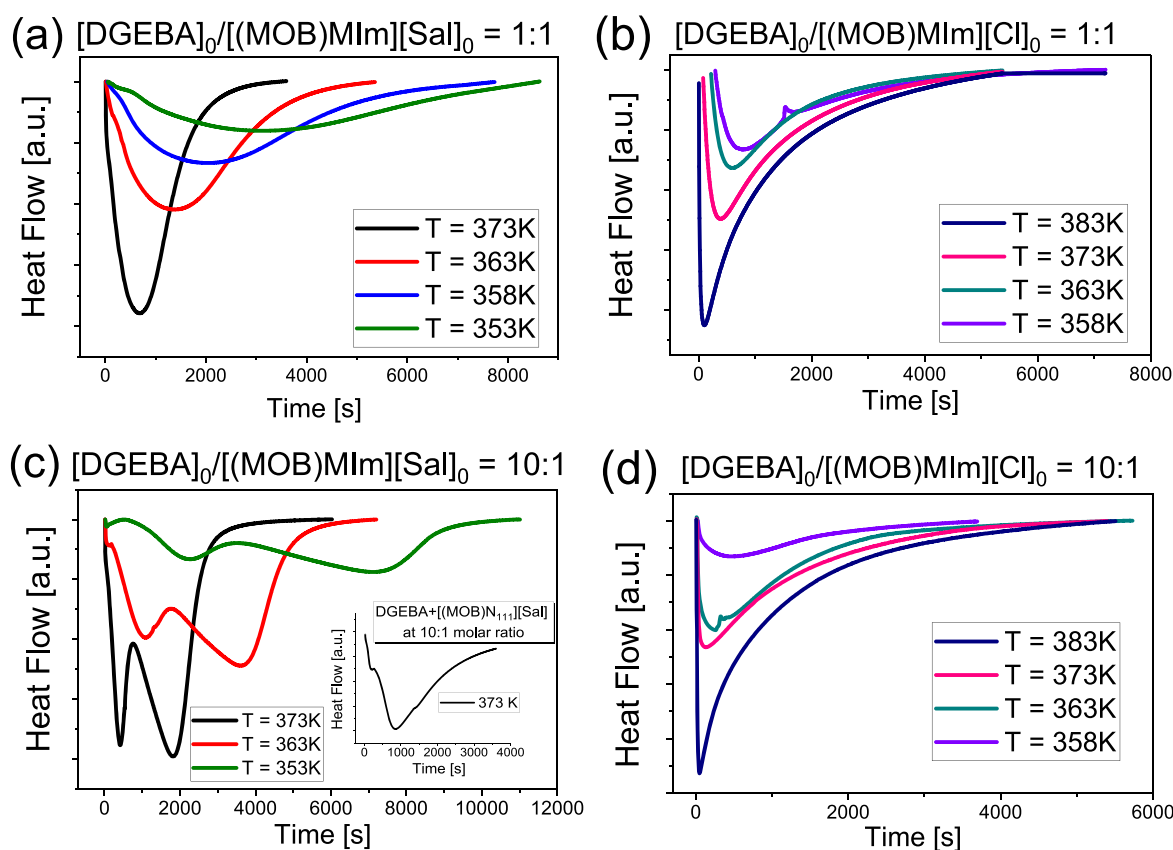
Figure 1. Representative DSC thermograms obtained upon the curing of DGEBA with $[(MOB)MIm][Sal]$ (a, c) and $[(MOB)MIm][Cl]$ (b, d) mixed at two molar ratios (1:1 and 10:1) at various reaction temperatures, $T_{reaction} = 353-383$ K. Moreover, for comparison, the inset in (c) contains a DSC thermogram of the DGEBA cured with ionic liquid having different cation $[(MOB)N_{111}][Sal]$ at the same $[DGEBA]_0/IL_0 = 10:1$ molar ratio.

independently of the concentration of $[(MOB)MIm][Cl]$. A similar sharp monomodal exothermic peak was also previously reported for the curing of DGEBA with 1-(3-aminopropyl)-3-butylimidazolium bis(trifluoromethylsulfonyl)imide (assigned as $[apbim][NTf_2]$).[33]

Interestingly, both DGEBA/IL systems studied herein revealed a notable different curing characteristic. Thus, the following questions arise: Why does the two-step curing occur in the case of PS I with low IL concentration? Is it related to the type of used anion (salicylate)? Briefly, it is worthwhile to stress that the multistage reactions are often closely linked to the presence of some anions, dicyanamide $[N(CN)_2]$,[42,43] thiocyanate $[SCN]$,[44] acetate $[OAc]$,[45] or phosphinate,[5] as well as halogen anions (chloride, $[Cl]$, or iodide, $[I]$),[46,47] combined with the imidazole cation. Some insight into this issue provided investigations on the curing of epoxy–phenol resin with either 1,2,4- or 2,4-substituted imidazole derivatives, where authors postulated to link the existence of additional steps in thermograms with the formation of the exothermic adduct by the imidazole moiety.[48−50] Nevertheless, one must remember that in both systems studied herein the imidazolium-based cation was applied, and reactions were performed at temperatures much lower with respect to those examined in ref 48. Thus, considering these facts, one can suppose that the explanation given by Heise et al.[48−50] cannot be used to understand our data. Anyway, to test this possibility and rule out the possible thermal decomposition of ILs during curing, which might strongly affect the mechanism and character of this reaction,[42] further DSC investigations were

carried out. In Figure S1, we have presented thermograms collected upon heating of $[(MOB)MIm][Sal]$ and $[(MOB)MIm][Cl]$ from room temperature up to $T = 573$ K. It was found that in the former and latter compound endothermal ($T = 500$ K) and exothermal ($T = 490$ K) processes indicating their possible thermal degradation are observed, respectively. However, it is important to note that these characteristic transitions are located much above temperatures at which isothermal curing of DGEBA with both ionic liquids was studied ($T = 353-383$ K). Hence, even though there might be some side reactions occurring within curing of an epoxy resin with ILs, which, as reported in the literature, might be triggered by the presence of bases, heating, and hydroxyl anions,[42,51] their impact on the progress of curing is negligible or marginal.

Thus, to find out the origin of the peculiar curing kinetics in the system consisting of DGEBA and $[(MOB)MIm][Sal]$, further experiments with the IL hardener possesing the quaternary ammonium cation (1-butoxymethyl-1-methyl)-trimethylammonium and salicylate anion (labeled as $[(MOB)N_{111}][Sal]$) were performed (see the inset in Figure 1c). The chemical structure of this ionic liquid is presented in Figure S3. Herein, it should be pointed out that, in contrast to the imidazolium-based cation, the $[(MOB)N_{111}]$ cation cannot initiate the curing process. Therefore, this simple experiment can be a direct evidence of the chemical activity of the salicylate anion once polymerization of DGEBA with $[(MOB)-N_{111}][Sal]$ is observed. In this context, it is worthwhile to add that salicylic acid, its derivatives (e.g., those containing halogen
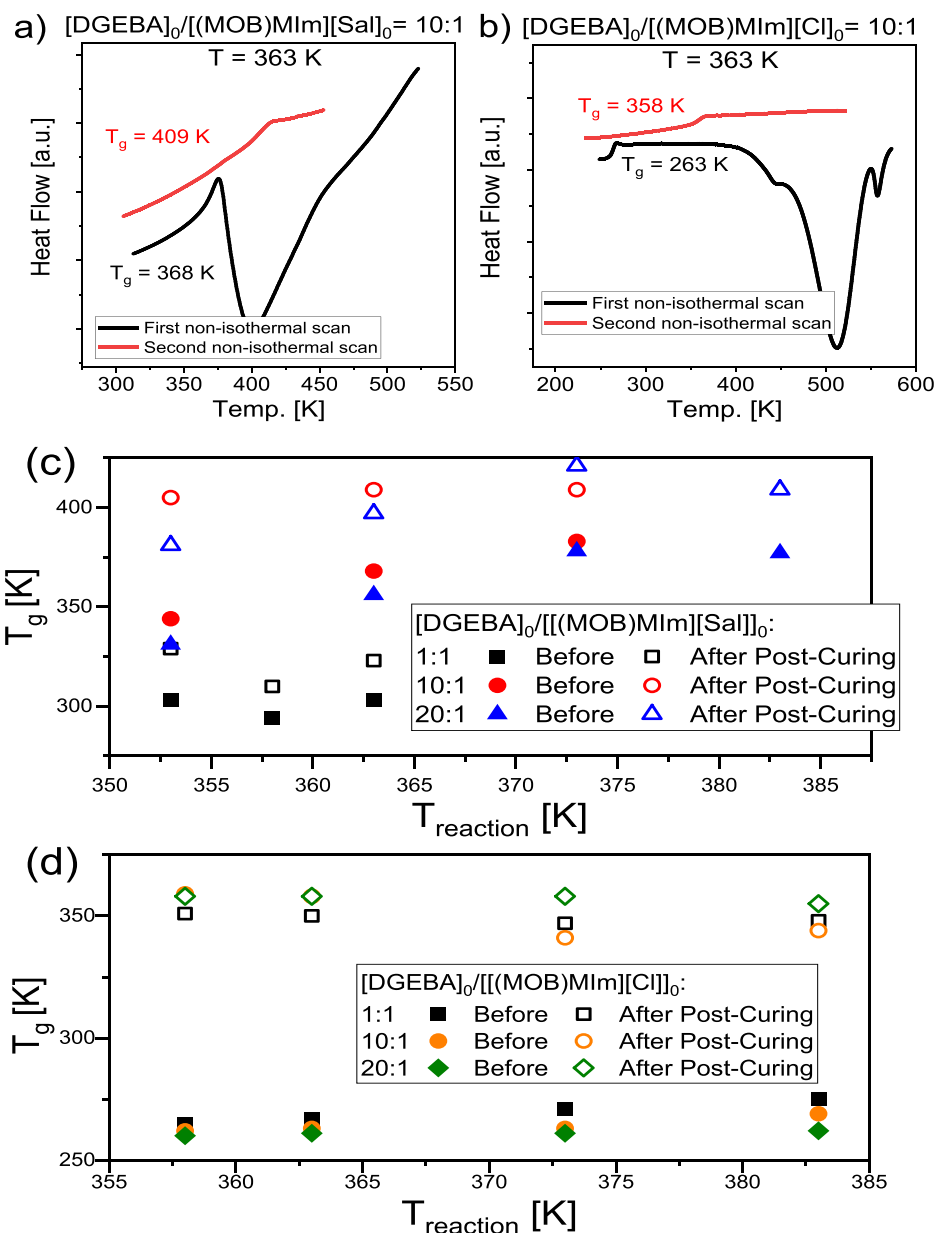
Figure 2. (a, b) Nonisothermal DSC thermograms obtained for $[DGEBA]_0/[(MOB)MIm][Sal]_0 = 10:1$ (a) and $[DGEBA]_0/[(MOB)MIm][Cl]_0 = 10:1$ (b), both previously isothermally cured at $T_{reaction} = 363$ K. (c, d) Evolution of T_g of polymerized epoxy resins obtained before and after nonisothermal scans for DGEBA/[(MOB)MIm][Sal] (c) and DGEBA/[(MOB)MIm][Cl] (d) at various molar ratios.

atoms) and salts, salicylates, are well-known accelerators applied for curing epoxy resins with amine-based hardeners.[52] Their effectiveness with respect to the nonaccelerated as well as accelerated by phenols, triphenyl phosphite, or tertiary amines curing process has been documented in the previous reports.[52,53]

What is more, the presence of salicylic acid also has a direct influence on the structure of the obtained resins through modification of the curing mechanism. This involves, for example, a reduction of ether bonds produced during epoxy hardening, in relation to those formed by primary and secondary amines.[54] However, simultaneously, the initiating activity of salicylates upon epoxy resin curing is much rarely investigated in the literature. As shown in the inset to Figure 1c for $[DGEBA]_0/[(MOB)N_{111}][Sal]_0 = 10:1$, simple curing kinetics is observed upon the isothermal annealing at $T_{reaction} =$

373 K, contrary to the main panel of Figure 1c, which demonstrates the respective thermograms obtained for the $[DGEBA]-[(MOB)MIm][Sal]$ composition at the same molar ratio that revealed bimodal kinetics. This clearly indicates that the peculiarity (double exothermic peak) found in the raw data presented in Figure 1c probably originates from the enhanced initiation properties of both the salicylate anion and the imidazolium-based cation. Note that the curing reaction of DGEBA with imidazolium-based ILs is generally a complex process comprising several different initiation pathways such as "carbene", "imidazole", and "counterion" routes.[40,45]

To investigate the kinetics of the curing process, as first, we have determined the monomer conversion, α, for the reactions performed at various temperatures for all systems studied herein. Although α can be estimated from many experimental techniques, i.e., nuclear magnetic resonance (NMR) as well as
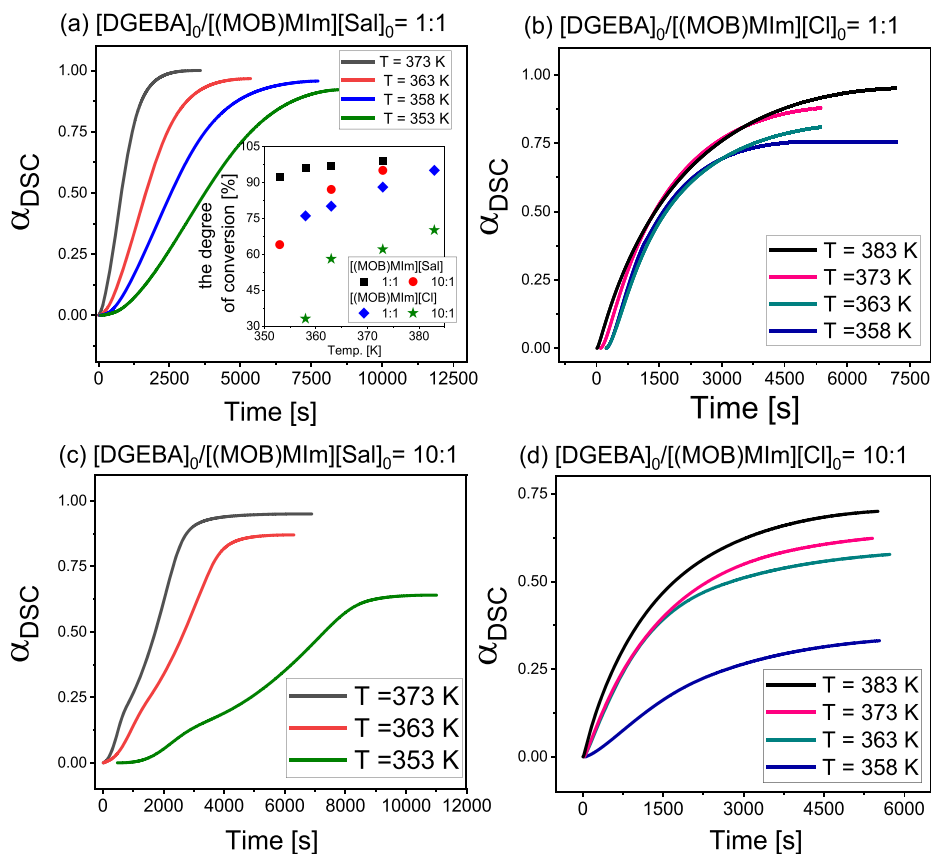
Figure 3. Time evolution of the DSC conversion, α_{DSC}, obtained for DGEBA/[(MOB)MIm][Sal] (a, c) and DGEBA/[(MOB)MIm][Cl] (b, d) at various molar ratios and temperature conditions.

Fourier transfer infrared (FTIR) and Raman spectroscopies,[40,41,55] one of the most suitable and commonly applied methods for following the conversion of epoxy resin upon the curing process is DSC.[39,56,57] Employing the well-established procedure, we estimated the calorimetric conversion, α_{DSC}, from the following equation:

$$\alpha_{DSC} = \frac{\Delta H_{(iso)}}{\Delta H_{total}} \quad\quad\quad (1)$$

where $\Delta H_{(iso)}$ is the enthalpy change as a function of the polymerization time at a given temperature (isothermal measurements), while ΔH_{total} is the total enthalpy of the studied reaction determined to be a sum of enthalpies from isothermal, $\Delta H_{(iso)}$, and nonisothermal, $\Delta H_{(non-iso)}$, experiments. Therefore, to estimate α_{DSC}, we have to calculate the value of $\Delta H_{(non-iso)}$. For that purpose, we performed additional dynamic (nonisothermal) DSC scans of isothermally (partially) polymerized samples. Representative nonisothermal DSC thermograms recorded for isothermally hardened (solid black lines) and fully cured systems (solid red lines) of the two investigated $[DGEBA]_0/[ILs]_0$ = 10:1 compositions are presented in Figure 2a,b.

As illustrated in Figure 2a,b, all isothermally polymerized samples measured as a function of temperature revealed the presence of (i) the endothermic process, corresponding to the glass transition, and (ii) a huge exothermic peak that originated from the polymerization of unreacted monomer present in the system (solid black lines). On the other hand, the fully cured epoxy resins exhibited only one characteristic endothermic

heat capacity jump (T_g) located at much higher temperatures with respect to those polymerized isothermally (solid red lines in Figure 2a,b). The evolutions of T_g recorded before and after the nonisothermal measurements are presented in Figure 2c,d. Interestingly, in the case of the PS I system, T_gs of both isothermally and fully cured materials estimated for $[DGEBA]_0/[(MOB)MIm][Sal]_0$ = 1:1 are much lower ($T_{g,isotherm} \sim 300$ K and $T_{g,cured} \sim 320$ K) than those prepared with the smaller content of IL ($T_{g,isotherm} \sim 350$ K and $T_{g,cured} \sim 400$ K, Figure 2c). However, they are significantly higher in relation to the second IL-based hardener ([(MOB)MIm]-[Cl]). Note that T_g of isothermally polymerized and cured DGEBA/[(MOB)MIm][Cl] systems reached $T_{g,isotherm} \sim 260$ K, and $T_{g,cured} \sim 350$ K, respectively (see Figure 2d). This might indicate that, most likely, the DGEBA/[(MOB)MIm]-[Sal] products are highly cross-linked polymers (high T_g), while hardening of the second system yields oligomeric linear polymers (low T_g). Moreover, it should be pointed out that all isothermally polymerized systems exhibit lower T_g values than the reaction temperature irrespective of the applied IL hardener. This effect is even more visible in the case of [(MOB)MIm][Cl]. One can recall that, generally, T_g of produced epoxy-based systems is comparable to the reaction temperature, $T_{reaction}$, due to the reduction of the monomer diffusion upon approaching T_g (which, in fact, is a limiting step of the process). Additionally, it can be stressed that the determined values of T_g of both isothermally polymerized and fully cured systems are either lower than or comparable to those ones reported in the literature. It can be noticed that the glass transition temperatures of epoxy resins cured with the

two 1,3-substituted imidazolium-based IL hardeners possessing different anions (including tetrafluoroborate $[BF_4]$, thiocyanate $[SCN]$, or dicyanamide $[N(CN)_2]$) reached T_g = 420–454 K,[42,47,58,59] whereas the combination of acetate/phosphonium cation and 2-ethylhexanoate/phosphonium cation as curing agents resulted in T_g varying between 434 and 417 K, respectively.[44,60]

After determining the values of $\Delta H_{(non-iso)}$, we estimated the DSC conversion, α_{DSC}, from eq 1. Herein it should be noted that considering that (i) isothermal reactions proceeded with the high monomer consumption and (ii) there is only partial overlapping of the residual heat of the reaction and heat of the IL's thermal decomposition occurring at very high temperatures, the latter process has a rather marginal impact on the calculated monomer conversion. The temperature dependence of calculated α_{DSC} is shown in the inset of Figure 3a. As illustrated, the application of $[(MOB)MIm][Sal]$ as the curing agent leads to a higher monomer conversion when compared to the other examined ionic hardener. Note that for the PS I system almost full DGEBA consumption ($\alpha_{DSC} \geq 90\%$) was reached independently of the IL's content. Comparable values of α_{DSC} were also calculated for PS II ($[DGEBA]_0/[(MOB)MIm][Cl]_0$ = 1:1). However, for this system, α_{DSC} strongly depends on IL's concentration. For example, in the case of $[DGEBA]_0/[IL]_0$ = 10:1, α_{DSC} decreases to ∼60% at $T_{reaction}$ = 383 K (see the inset in Figure 3a). It is worth mentioning that the final degree of monomer conversion depends on the structural features of the applied hardener and usually fluctuates between 40% and 60% in the case of an ionic curing agent.[5] Note that for cationic hardeners the monomer conversions were comparable to those obtained for the anionic ones, reaching values of 50–70%.[33] Interestingly, for some epoxy/ILs systems, after isothermal curing at low temperatures, extremely low monomer conversion ($\alpha \sim 3\%$) was obtained.[47] Nevertheless, for the epoxy/IL systems studied herein, calculated α_{DSC} are comparable to those previously reported for nonionic curing agents.[11] As demonstrated, the application of an imidazolium-based hardener with salicylate anion allows to reach higher conversion at comparable temperature conditions and IL's concentration. This indicates that the studied $[(MOB)MIm][Sal]$ hardener might be considered as a latent curing agent. On the other hand, it should be pointed out that in the case of $[DGEBA]_0/[IL]_0$ = 1:1 the same α_{DSC} was reached for the shorter time in the case of DGEBA/$[(MOB)MIm][Sal]$ than DGEBA/$[(MOB)MIm][Cl]$, which might suggest, in fact, the better catalytic activity of the salicylate anion.

Next, we plotted the determined α_{DSC} as a function of time for all investigated systems (see Figure 3). As shown, the type of curing agent/anion and its concentration have a crucial impact on the kinetics curves. For the PS I system ($[DGEBA]_0/[(MOB)MIm][Sal]_0$ = 1:1), a typical autocatalytic behavior, characterized by the S-shape, can be observed, whereas with the decreasing concentration of the hardener $[DGEBA]/[IL]$ to 10:1 yields two clearly visible steps. Note that this phenomenon is also observed, but not as spectacular as in the case of $[DGEBA]_0/[(MOB)MIm][Sal]_0$ = 20:1 (see Figure S4). One can recall that the detected S-shaped kinetic curves are generally reported for epoxy resin curing in the presence of the nonionic hardener, i.e., both aliphatic[11] and primary aromatic amines,[11,61] as a result of the two various curing steps characterized by different constant rates, k, and activation barriers, E_a. Briefly, the first one is related to the

noncatalyzed ring-opening with a ternary transition state of amine or by nucleophile attack (usually characterized by higher E_a). By contrast, the second one is believed to be a subsequent process connected to the autocatalytic ring-opening that involves alkoxide and epoxide groups, which may be catalyzed by the hydroxyl groups formed from the already opened oxirane rings.

On the other hand, the $\alpha_{DSC}(t)$ dependences estimated for the PS II system (DGEBA/$[(MOB)MIm][Cl]$) revealed an exponential-like behavior, characteristic of the first-order kinetics (see Figure 3b,d).[33,62] It should be noted that similar exponential kinetic curves were also previously reported for the curing of DGEBA with both 1-(3-aminopropyl)-3-butylimidazolium bis(trifluoromethylsulfonyl)imide and tetrabutylammonium leucine (assigned as $[apbim][NTf_2]$ and $[N_{4444}]$-$[Leu]$, respectively).[33] The first-order kinetics were discussed in terms of the polymerization mechanism change, related to the presence of IL hardener acting as both the initiator and the cocatalyst.[33] Therefore, the exponential kinetics of studied DGEBA/$[(MOB)MIm][Cl]$ systems might also result from the increased catalytic properties of the applied chloride IL curing agent. Hence, as shown and discussed above, the application of imidazole hardeners with different anions affects the polymerization kinetics in various ways.

To get deeper insights into the examined curing kinetics, we analyzed the obtained experimental data with available phenomenological kinetic models. Taking into account a complex and bimodal character of the hardening process, one can stress that applications of mechanistic models would be a challenging task. Fortunately, one can apply phenomenological ones, which can be used without the identification of the species involved in the reactions. This approach is frequently explored in the literature, where different model-free[63] and model-fitting[64] methods are commonly applied to study the kinetics of a variety of epoxy resins. The former group is represented by, i.e., the Friedman, Flynn–Wall–Ozawa, and Kissinger–Akahira–Sunose methods, whereas the latter ones are based on model-fitting algorithms, that are the nth order, Avrami, and the autocatalytic model (Kamal model[65] and its modifications[66]).[67] However, we would like to highlight that both types of methods are used mostly to characterize the standard kinetic curve (characterized by the one exothermic process), which precludes their use in a description of the data presented in Figure 3c.

Nevertheless, we previously demonstrated that the original Kamal model or its modified version can be successfully applied to describe the autocatalytic behavior of epoxy curing in the presence of classical aromatic amine–aniline, even in a broad range of thermodynamic conditions.[12] Therefore, the Kamal equation has been chosen as a first approach to determining the kinetics parameters describing the progress of a reaction:[68]

$$\frac{d\alpha}{dt} = (k_1 + k_2\alpha^m)(1 - \alpha)^n \tag{2}$$

where α is a degree of thermal conversion, k_1 and k_2 correspond to noncatalyzed and catalyzed reaction rate constants, and m and n are the model constants. The application of this model provides reasonably good fits to the experimental data over the entire range of temperatures for $[DGEBA]_0/[(MOB)MIm][Sal]_0$ = 1:1. This is evidenced by the representative example in Figure S5. However, in the case of systems with low IL content ($[DGEBA]_0/[IL]_0$ = 10:1 and

$[DGEBA]_0/[IL]_0 = 20:1)$, the shape of $d\alpha/dt$ vs α became much more complex, as is clearly demonstrated in the inset of Figure 4b. As shown, two evident peaks are visible, which
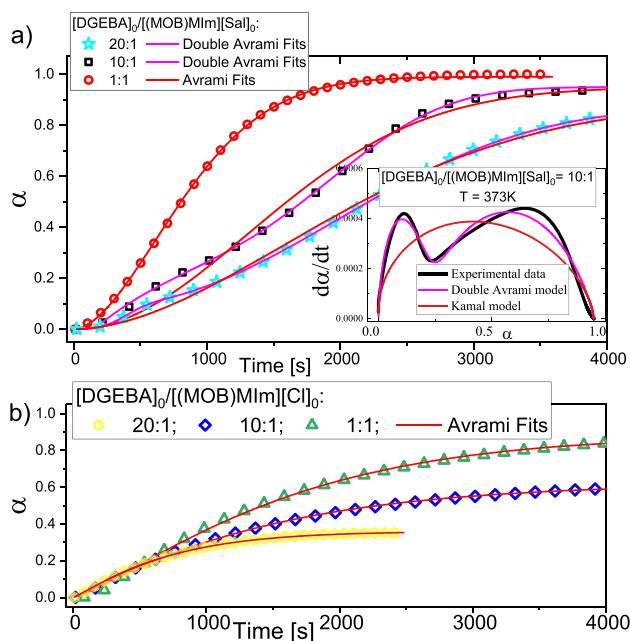

Figure 4. Experimental data of the real conversion of DGEBA/ [(MOB)MIm][Sal] (a) and DGEBA/[(MOB)MIm][Cl] (b) mixed at various molar ratios and polymerized at $T = 373$ K. As the inset in (a), the $d\alpha/dt$ plotted as a function of α are shown. Solid lines present a fitting line constructed from the kinetics parameters obtained from the Kamal (red) and Avrami (purple) models.

confirms the previous assumption that we are dealing with two curing stages. Probably, the first one is directly linked to the combined imidazolium salicylate activity effect, participating as an initiator and a cocatalyst. According to the applied amount of ionic liquid, DGEBA is fully or partially cured in the case of a 1:1 or 10:1 (and 20:1) molar ratio mixture, respectively. In the latter situation, the initial catalytic effect observed at the beginning of curing, after the primary step, is reduced, which is reflected in a decrease of $d\alpha/dt$. Nevertheless, as the initial stage of curing proceeds with the epoxide ring-opening, newly hydroxyl groups with the catalytic activity are formed. Simultaneously, the imidazole cation activity should still be accessible. As a consequence, the reaction is accelerated to the second peak maximum. Then, the final decrease of the reaction rate is caused by the reduction of monomer concentration and suppressed diffusion.

An analysis of the initial stage of the curing process registered for the $[DGEBA]_0/[(MOB)MIm][Sal]_0$ mixed in 10:1 molar ratio was performed. This enabled us to determine the k_1 parameter in the model-independent way.[12] Subsequently, we fitted the Kamal model to the experimentally obtained dependence of $d\alpha/dt$ vs α. From Figure 4a, it can be seen that this approach does not fit the experimental data measured for this system correctly, even though it accounts for the two-step mechanism of the reaction. Consequently, further analysis of the curing processes, especially for $[DGEBA]_0/$ $[(MOB)MIm][Sal]_0 = 10:1$ and $[DGEBA]_0/[(MOB)MIm]$-$[Sal]_0 = 20:1$, requires the employment of the different model.

To find a solution to this problem and maintain consistency between the constant rates determined for various systems, we decided to exclude the Kamal model from further considerations. Instead, we chose the Avrami approach,[69−71] which many researchers—including some of us—had successfully applied to study the overall progress of curing.[72−74] It should
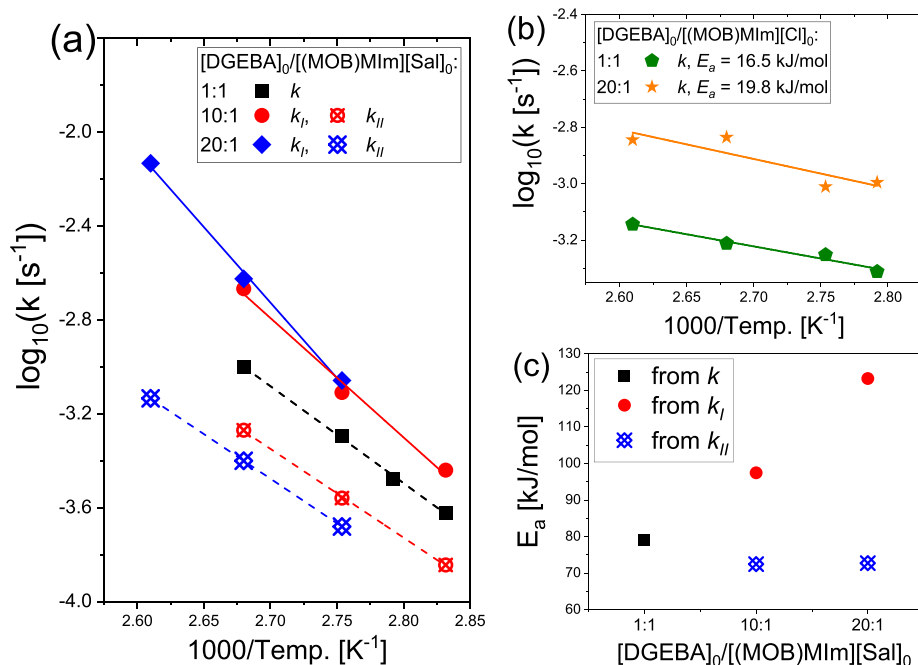

Figure 5. (a, b) Temperature dependence of reaction constant rates determined from the isothermal polymerization of DGEBA/ [(MOB)MIm][Sal] (a) and DGEBA/[(MOB)MIm][Cl] (b) systems. (c) Activation energies calculated for DGEBA/[(MOB)MIm][Sal] compositions from the Arrhenius equation (eq 5).

be stressed that because of its simplicity, the Avrami model seems to be the perfect choice for the further modification. Few attempts of that type of approach can be found in the literature.[75−77] Using the classical Avrami eq 3

$$\alpha(t) = C - e^{(-kt^n)} \qquad (3)$$

for the systems ($[DGEBA]_0/[(MOB)MIm][Cl]_0$ mixed in the following molar ratios 20:1, 10:1, and 1:1 and equimolar composition of [DGEBA] and [[(MOB)MIm][Sal]] polymerized at $T = 373$ K), we calculated parameters k and n, which are the temperature-dependent reaction rate and Avrami exponent, respectively. The obtained results are presented in Figure 4 and Figure 5. Subsequently, we propose the following modification of the Avrami model to consider two-stages of curing (herein named "double Avrami" model):

$$\alpha(t) = C - x \exp(-(k_I t)^m) - (C - x) \exp(-(k_{II} t)^n) \qquad (4)$$

where C is a final (real) conversion, k_I and k_{II} are the reaction rate constants (note that they have nothing to do with k_1 and k_2, which can be obtained from the Kamal model), x parametrizes the relative contributions of each reaction step, and m and n are the fit parameters. Note that the data analysis with the "double Avrami" model yields two reaction rates (k_I and k_{II}), which herein are assigned to the first and second stages of the studied curing process, respectively. Interestingly, contrary to the Kamal and classical Avrami approaches, the use of the "double Avrami" model leads to a satisfactory description of the curing process performed with the use of [(MOB)MIm][Sal] for different $[DGEBA]_0/[IL]_0$ concentrations (see Figure 4a). Additionally, in the inset of Figure 4a, we presented the predicted by the "double Avrami" model dependence of da/dt vs a. In this case, the two evident peaks are described by the fits with satisfactory accuracy. Hence, we can conclude that the "double Avrami" model describes the overall curing kinetics ($[DGEBA]_0/[(MOB)MIm][Sal]_0 =$ 10:1 and 20:1) much better than the Kamal model does.

The determined values of the constant rates k describing curing DGEBA with both ionic liquids [(MOB)MIm][Sal] and [(MOB)MIm][Cl] are presented in Figures 5a and 5b, respectively. Note that in the case of the 10:1 and 20:1 molar ratios of the DGEBA/[(MOB)MIm][Sal] compositions analysis of the kinetic curves with the use of double Avrami model yields two different rates, labeled herein as k_I and k_{II}, whereas for the other systems, only one k was estimated. As shown, the estimated constant rates increase linearly with the curing temperature and increasing concentration of ILs. However, the constant rates of DGEBA/[(MOB)MIm][Sal] systems increase with increasing temperature more dramatically as compared to PS II.

Further insight into the kinetics of both stages of reactions can be gained by a comparison of activation energies, E_a, which can be estimated by using the Arrhenius equation:

$$k = k_0 \exp\left(\frac{E_a}{RT}\right) \qquad (5)$$

where k_0 is a pre-exponential factor and R is the universal gas constant. The determined values of E_a are presented in Figure 5. It was found that $E_{a,I} = 97.4$ kJ/mol and $E_{a,I} = 123.2$ kJ/mol as well as $E_{a,II} = 72.4$ kJ/mol and $E_{a,II} = 72.7$ kJ/mol for DGEBA mixed with [(MOB)MIm][Sal] in the 10:1 and 20:1 molar ratios, respectively (Figure 5c). As one can expect, the

activation energies for the initial stage of curing, marked as $E_{a,I}$, are higher in comparison to $E_{a,II}$, which is consistent with the literature data.[33] Moreover, the activation energy of the first stage is correlated to the content of [(MOB)MIm][Sal]. As a consequence, a decrease in IL's concentration results in an increase in the activation energy of the first step of curing ($E_{a,I}$). By contrast, it did not affect the activation barrier of the second stage of the process (Figure 5c). Furthermore, in the case of high ionic liquid loading, $[DGEBA]_0/[IL]_0 = 1:1$, we can assume that nearly all of the epoxy groups were catalytically consumed; therefore, the quite low E_a, equal to 79.1 kJ/mol, was estimated. On the other hand, the $k(T)$ dependences for the second system studied herein, DGEBA/[(MOB)MIm][Cl], and the corresponding estimated activation energies are shown in Figure 5b. As presented, $E_a = 16.5$ and 19.8 kJ/mol for $[DGEBA]_0/[IL]_0 = 1:1$ and $[DGEBA]_0/[IL]_0 = 20:1$, respectively. It should be pointed out that they are much lower in comparison to those calculated for cation with salicylic anion. Although only a few literature reports discuss the activation barrier for epoxy resin cured with ionic liquids, it should be highlighted that our values are consistent with the results previously presented by Maksym et al.[33] and Binks et al.[78] As an example, one can mention ionic liquid with imidazolium-based cation for which the reported activation energy is $E_a = 19$ kJ/mol.[33] Moreover, the activation barriers $E_a = 72.7$ and 72.4 kJ/mol estimated for curing DGEBA with [(MOB)IM][Sal] are in perfect agreement with the respective value for the system reported in ref 78 (where $E_a = 74$ kJ/mol). As shown, the values of E_a are closely connected to the applied monomers, which also affect the dominant curing mechanism. One can expect that due to a common presence of imidazolium-based cation, both studied systems polymerize according to a similar mechanism (probably via "carben" and "imidazole" routes). However, in the case of DGEBA/[(MOB)IM][Sal], additionally, the "counterion" route might be favored.

Finally, we examined the relationship between the structure of networked epoxy resins, a type of anion, the applied amount of ILs, and the conductivity of fully cured resins. As mentioned in the Introduction, these parameters are unquestionably important for achieving significant progress in energy storage, i.e., to design and produce flexible, solid electrolytes, or separation membranes for Li-ion batteries.[25] Herein, we measured the ionic conductivity, σ_{dc}, of produced resins by means of broadband dielectric spectroscopy (BDS) at T_g, which were previously determined from dynamic DSC experiments. We should highlight that measuring σ_{dc} of all cured materials at T_g allows for the comparing of systems characterized by the same viscosity and molecular mobility, independent of their structure.[79] The determined σ_{dc} conductivity at their glass transition temperatures for $[DGEBA]_0/[(MOB)MIm][Sal]_0 = 1:1$ and $[DGEBA]_0/[(MOB)MIm][Sal]_0 = 10:1$ was equal to $\sigma_{dc} = 7.18 \times 10^{-14}$ S/cm and $\sigma_{dc} = 1.05 \times 10^{-15}$ S/cm at T_g, respectively. On the other hand, for $[DGEBA]_0/[(MOB)MIm][Cl]_0 = 1:1$ and $[DGEBA]_0/[(MOB)MIm][Cl]_0 = 10:1$, much higher values, $\sigma_{dc} = 6.1 \times 10^{-10}$ S/cm and $\sigma_{dc} = 1.82 \times 10^{-10}$ S/cm at T_g, were reported. The obtained σ_{dc} are lower than those presented in the literature, i.e., for 1-decyl-3-methyl-imidazolium bromide [DMIm][Br], where $\sigma_{dc} = 10^{-6}$ S/cm at room temperature and $\sigma_{dc} = 10^{-3}$ S/cm at $T = 443$ K,[24] where the cation part of ILs is covalently linked to the epoxy network to a considerably lower degree. Even higher

conductivity was achieved for 1-ethyl-3-methylimidazolium bis(trifluoromethanesulfonyl)imide ([EMIm][TFSI]) added to the mixture of DGEBA and tetrafunctional epoxy resins.[80] Note that in the discussed cases IL-based hardeners were applied together with the classical nonconducting ones. Moreover, one can also find studies indicating the implementation of ionic groups into networked resin due to the application of ionic monomers (or comonomers) via polyaddition polymerization. In this context, one can notice the diepoxy-functionalized 1,2,3-triazolium ionic liquid[35] and glycidyltrimethylammonium bis(trifluoromethanesulfonyl)-imide (GTMATFSI),[32] which were successfully polymerized to achieve an epoxy network structure with built-in cations and movable anions resulting in a relatively high conductivity, σ_{dc} = 2 × 10^{-7} S/cm (at T = 303 K[35]) and $\sigma_{dc} \sim 10^{-3}-10^{-5}$ S/m,[32] respectively. It is also worth mentioning that slightly lower values of conductivity were obtained for epoxy resin-based polycations and polyanions, where σ_{dc} = 5 × 10^{-8} and σ_{dc} = 3 × 10^{-8} S/cm at T_g for DGEBA + [apbim][NTf$_2$] and DGEBA + [N$_{4444}$][Leu], respectively.[33] The conductivity of the mentioned examples of epoxy resin-based conductive materials differs significantly, probably due to differences in the chemical structure of the produced network and mobility or the viscosity of the studied materials,[32,81] which strongly affects the charge transport mechanism.[82,83] At this point, it should also be stressed that very often the determined values of σ_{dc} are reported for different temperature conditions, as there is no unifying protocol to present them in a comparable manner. Most of the reports devoted to ionic-based epoxy resins listed values of σ_{dc} measured at room temperature (~293−303 K), which, for various cases, indicates a totally different system viscosity, ion mobility, and dc conductivity. To avoid any misunderstandings, herein, we measured σ_{dc} of all cured materials at T_g, which allows for the comparing of systems characterized by the same viscosity and molecular mobility, irrespective of their structure. As shown, the PS II system (DGEBA/[(MOB)MIm][Cl]) is characterized by much higher conductivity, probably due to the presence of the polar and highly mobile chloride anion, which cannot be built into the polymer structure. Moreover, this kind of polymerization most likely yields oligomeric linear polymers (low T_g) that contribute to enhanced conductivity. On the other hand, in the case of the second system studied herein, a product is a highly cross-linked polymer (high T_g), where the mobility of the ions is highly restricted.

4. CONCLUSION

Herein, we studied the isothermal cure kinetics of DGEBA in the presence of imidazolium-based ILs hardeners containing different anions, that is, a salicylate and chloride, denoted as [(MOB)MIm][Sal] and [(MOB)MIm][Cl], respectively. The curing process of epoxy/IL systems was investigated at different (moderate) temperatures through the use of various initial molar ratios of DGEBA/IL. Performed calorimetric experiments for [DGEBA]$_0$/[(MOB)MIm][Sal]$_0$ = 10:1 and [DGEBA]$_0$/[(MOB)MIm][Sal]$_0$ = 20:1 allowed us to demonstrate that there are two peaks in the thermograms upon the isothermal curing. This phenomenon might be probably assigned to the promoted initiation by the anion (salicylate)−cation (imidazolium-based) combination, whereas in the case of [(MOB)MIm][Cl], only one hardening step was observed. The detailed kinetic analysis performed through the application of the modified Avrami model provided constant

reaction rates that enabled us to further calculate activation energies for the curing process for all the systems studied herein. It should be pointed out that we applied a combination of two Avrami equations (assigned by us as "double Avrami") to describe the two-step kinetics of DGEBA/[(MOB)MIm]-[Sal]. As observed, the proposed approach works perfectly. Interestingly, the reactions performed in the presence of IL with the salicylate anion are shorter, even though they are characterized by much higher activation energies, with respect to those consisting of the chloride anion. Thus, it seems that in the DGEBA/[(MOB)MIm][Sal] composition the presence of the salicylate anion leads to an additional initiation of epoxy ring-opening, which is absent in the case of chloride anion. Moreover, DGEBA/[(MOB)MIm][Cl] systems have a lower glass transition temperature, T_g, than the second system independently of the applied IL concentration. This might indicate that, most likely, DGEBA/[(MOB)MIm][Sal] products are highly cross-linked polymers (high T_g), while those consisting of DGEBA/[(MOB)MIm][Cl] are oligomeric linear polymers (low T_g). However, the latter systems are characterized by significantly higher conductivity (measured at the calorimetric glass transition temperature, T_g), probably due to the presence of polar and highly mobile chloride anion and oligomeric cations. Our data clearly presented that the type of anion has a crucial impact on the polymerization mechanism, kinetics, and properties of produced materials.

■ ASSOCIATED CONTENT

Ⓢ Supporting Information

The Supporting Information is available free of charge at https://pubs.acs.org/doi/10.1021/acs.macromol.0c00783.

Experimental details; Figures S1−S5 (PDF)

■ AUTHOR INFORMATION

Corresponding Authors

Andrzej Dzienia − *Institute of Chemistry and Silesian Center of Education and Interdisciplinary Research, University of Silesia, 40-006 Katowice, Poland;* ⓘ orcid.org/0000-0002-9628-0224; Email: andrzej.dzienia@smcebi.edu.pl

Kamil Kamiński − *Institute of Physics and Silesian Center of Education and Interdisciplinary Research, University of Silesia, 41-500 Chorzow, Poland;* ⓘ orcid.org/0000-0002-5871-0203; Email: kamil.kaminski@us.edu.pl

Authors

Magdalena Tarnacka − *Institute of Physics and Silesian Center of Education and Interdisciplinary Research, University of Silesia, 41-500 Chorzow, Poland;* ⓘ orcid.org/0000-0002-9444-3114

Kajetan Koperwas − *Institute of Physics and Silesian Center of Education and Interdisciplinary Research, University of Silesia, 41-500 Chorzow, Poland;* ⓘ orcid.org/0000-0003-2359-5783

Paulina Maksym − *Institute of Physics and Silesian Center of Education and Interdisciplinary Research, University of Silesia, 41-500 Chorzow, Poland;* ⓘ orcid.org/0000-0002-8506-7102

Andrzej Zięba − *Department of Organic Chemistry, Faculty of Pharmaceutical Sciences in Sosnowiec, Medical University of Silesia in Katowice, 41-200 Sosnowiec, Poland*

Joanna Feder-Kubis − *Faculty of Chemistry, Wrocław University of Science and Technology, 50-370 Wrocław, Poland;* ◉ orcid.org/0000-0002-2883-8556

Marian Paluch − *Institute of Physics and Silesian Center of Education and Interdisciplinary Research, University of Silesia, 41-500 Chorzow, Poland*

Notes

The authors declare no competing financial interest.

■ REFERENCES

(1) Jeon, H.; Park, J.; Shon, M. Corrosion Protection by Epoxy Coating Containing Multi-Walled Carbon Nanotubes. *J. Ind. Eng. Chem.* **2013**, *19* (3), 849−853.

(2) Miao, X.; Xing, A.; Yang, W.; He, L.; Meng, Y.; Li, X. Synthesis and Characterization of Hyperbranched Polyether/DGEBA Hybrid Coatings. *React. Funct. Polym.* **2018**, *122*, 116−122.

(3) Kumar, S.; Krishnan, S.; Samal, S. K.; Mohanty, S.; Nayak, S. K. Toughening of Petroleum Based (DGEBA) Epoxy Resins with Various Renewable Resources Based Flexible Chains for High Performance Applications: A Review. *Ind. Eng. Chem. Res.* **2018**, *57* (8), 2711−2726.

(4) Altuna, F. I.; Ruseckaite, R. A.; Stefani, P. M. Biobased Thermosetting Epoxy Foams: Mechanical and Thermal Characterization. *ACS Sustainable Chem. Eng.* **2015**, *3* (7), 1406−1411.

(5) Nguyen, T. K. L.; Livi, S.; Soares, B. G.; Pruvost, S.; Duchet-Rumeau, J.; Gérard, J. F. Ionic Liquids: A New Route for the Design of Epoxy Networks. *ACS Sustainable Chem. Eng.* **2016**, *4* (2), 481−490.

(6) Garcia, F. G.; Leyva, M. E.; Oliveira, M. G.; De Queiroz, A. A. A.; Simões, A. Z. Influence of Chemical Structure of Hardener on Mechanical and Adhesive Properties of Epoxy Polymers. *J. Appl. Polym. Sci.* **2010**, *117* (4), 2213−2219.

(7) De Nograro, F. F.; Guerrero, P.; Corcuera, M. A.; Mondragon, I. Effects of Chemical Structure of Hardener on Curing Evolution and on the Dynamic Mechanical Behavior of Epoxy Resins. *J. Appl. Polym. Sci.* **1995**, *56* (2), 177−192.

(8) Chattopadhyay, D. K.; Panda, S. S.; Raju, K. V. S. N. Thermal and Mechanical Properties of Epoxy Acrylate/Methacrylates UV Cured Coatings. *Prog. Org. Coat.* **2005**, *54* (1), 10−19.

(9) Tanrattanakul, V.; Jaroendee, D. Comparison between Microwave and Thermal Curing of Glass Fiber-Epoxy Composites: Effect of Microwave-Heating Cycle on Mechanical Properties. *J. Appl. Polym. Sci.* **2006**, *102* (2), 1059−1070.

(10) Tarnacka, M.; Dulski, M.; Starzonek, S.; Adrjanowicz, K.; Mapesa, E. U.; Kaminski, K.; Paluch, M. Following Kinetics and Dynamics of DGEBA-Aniline Polymerization in Nanoporous Native Alumina Oxide Membranes - FTIR and Dielectric Studies. *Polymer* **2015**, *68*, 253−261.

(11) Tarnacka, M.; Wikarek, M.; Pawlus, S.; Kaminski, K.; Paluch, M. Impact of High Pressure on the Progress of Polymerization of DGEBA Cured with Different Amine Hardeners: Dielectric and DSC Studies. *RSC Adv.* **2015**, *5* (128), 105934−105942.

(12) Dzienia, A.; Koperwas, K.; Tarnacka, M.; Chorąewski, M.; Postnikov, E. B.; Lowe, A. R.; Kamiński, K.; Paluch, M. Direct Insight into the Kinetics of the High-Pressure Step-Growth Polymerization of DGEBA/Aniline Model System. *Polymer* **2019**, *172*, 322−329.

(13) Pascault, J.-P.; Williams, R. J. J. In *Epoxy Polymers: New Materials and Innovations*; Wiley-VCH Verlag GmbH & Co. KGaA: Weinheim, Germany, 2010; Chapter 1, pp 1−12.

(14) Jin, F.-L.; Li, X.; Park, S.-J. Synthesis and Application of Epoxy Resins: A Review. *J. Ind. Eng. Chem.* **2015**, *29*, 1−11.

(15) Paluvai, N. R.; Mohanty, S.; Nayak, S. K. Synthesis and Modifications of Epoxy Resins and Their Composites: A Review. *Polym.-Plast. Technol. Eng.* **2014**, *53* (16), 1723−1758.

(16) Saurín, N.; Sanes, J.; Carrión, F. J.; Bermúdez, M. D. Self-Healing of Abrasion Damage on Epoxy Resin Controlled by Ionic Liquid. *RSC Adv.* **2016**, *6* (43), 37258−37264.

(17) Jin, H.; Mangun, C. L.; Stradley, D. S.; Moore, J. S.; Sottos, N. R.; White, S. R. Self-Healing Thermoset Using Encapsulated Epoxy-Amine Healing Chemistry. *Polymer* **2012**, *53* (2), 581−587.

(18) Liu, Y.; Han, C.; Tan, H.; Du, X. Thermal, Mechanical and Shape Memory Properties of Shape Memory Epoxy Resin. *Mater. Sci. Eng., A* **2010**, *527* (10−11), 2510−2514.

(19) Xie, T.; Rousseau, I. A. Facile Tailoring of Thermal Transition Temperatures of Epoxy Shape Memory Polymers. *Polymer* **2009**, *50* (8), 1852−1856.

(20) Maka, H.; Spychaj, T.; Zenker, M. High Performance Epoxy Composites Cured with Ionic Liquids. *J. Ind. Eng. Chem.* **2015**, *31*, 192−198.

(21) Jia, Q. M.; Li, J. B.; Wang, L. F.; Zhu, J. W.; Zheng, M. Electrically Conductive Epoxy Resin Composites Containing Polyaniline with Different Morphologies. *Mater. Sci. Eng., A* **2007**, *448* (1−2), 356−360.

(22) Sancaktar, E.; Bai, L. Electrically Conductive Epoxy Adhesives. *Polymers (Basel, Switz.)* **2011**, *3* (1), 427−466.

(23) Leclère, M.; Bernard, L.; Livi, S.; Bardet, M.; Guillermo, A.; Picard, L.; Duchet-Rumeau, J. Gelled Electrolyte Containing Phosphonium Ionic Liquids for Lithium-Ion Batteries. *Nanomaterials* **2018**, *8* (6), 435.

(24) Oliveira da Silva, L. C.; Soares, B. G. New All Solid-State Polymer Electrolyte Based on Epoxy Resin and Ionic Liquid for High Temperature Applications. *J. Appl. Polym. Sci.* **2018**, *135* (9), 45838.

(25) Vashchuk, A.; Fainleib, A. M.; Starostenko, O.; Grande, D. Application of Ionic Liquids in Thermosetting Polymers: Epoxy and Cyanate Ester Resins. *eXPRESS Polym. Lett.* **2018**, *12* (10), 898−917.

(26) Kaur, G.; Adhikari, R.; Cass, P.; Bown, M.; Gunatillake, P. Electrically Conductive Polymers and Composites for Biomedical Applications. *RSC Adv.* **2015**, *5* (47), 37553−37567.

(27) Simitzis, J.; Triantou, D.; Soulis, S. Binary Conducting Copolymers Based on Benzene, Biphenyl, Thiophene and Pyrrole. In *Conducting Polymers: Synthesis, Properties and Applications*; Nova Science Publishers: 2013; pp 27−52.

(28) Yuan, J.; Mecerreyes, D.; Antonietti, M. Poly(Ionic Liquid)s: An Update. *Prog. Polym. Sci.* **2013**, *38* (7), 1009−1036.

(29) Green, M. D.; Long, T. E. Designing Imidazole-Based Ionic Liquids and Ionic Liquid Monomers for Emerging Technologies. *Polym. Rev.* **2009**, *49* (4), 291−314.

(30) Gu, H.; Ma, C.; Gu, J.; Guo, J.; Yan, X.; Huang, J.; Zhang, Q.; Guo, Z. An Overview of Multifunctional Epoxy Nanocomposites. *J. Mater. Chem. C* **2016**, *4* (25), 5890−5906.

(31) Vashchuk, A.; Fainleib, A.; Starostenko, O.; Grande, D. Ionic Liquids and Thermosetting Polymers: A Critical Survey. *Polim. Zh.* **2018**, *40* (1), 3−15.

(32) Matsumoto, K.; Endo, T. Synthesis of Ion Conductive Networked Polymers Based on an Ionic Liquid Epoxide Having a Quaternary Ammonium Salt Structure. *Macromolecules* **2009**, *42* (13), 4580−4584.

(33) Maksym, P.; Tarnacka, M.; Dzienia, A.; Matuszek, K.; Chrobok, A.; Kaminski, K.; Paluch, M. Enhanced Polymerization Rate and Conductivity of Ionic Liquid-Based Epoxy Resin. *Macromolecules* **2017**, *50* (8), 3262−3272.

(34) Vashchuk, A.; Fainleib, A. M.; Starostenko, O.; Grande, D. Application of Ionic Liquids in Thermosetting Polymers: Epoxy and Cyanate Ester Resins. *eXPRESS Polym. Lett.* **2018**, *12* (10), 898−917.

(35) Ly Nguyen, T. K.; Obadia, M. M.; Serghei, A.; Livi, S.; Duchet-Rumeau, J.; Drockenmuller, E. 1,2,3-Triazolium-Based Epoxy-Amine Networks: Ion-Conducting Polymer Electrolytes. *Macromol. Rapid Commun.* **2016**, *37* (14), 1168−1174.

(36) Agmon, N. The Grotthuss Mechanism. *Chem. Phys. Lett.* **1995**, *244* (5−6), 456−462.

(37) Marx, D. Proton Transfer 200 Years after Von Grotthuss: Insights from Ab Initio Simulations. *ChemPhysChem* **2006**, *7* (9), 1848−1870.

(38) Ma, X.; Zeng, Y.; Wang, J.; Chen, P.; Liu, S.; Xiong, X.; Ren, R.; Xiong, X. Isothermal Curing Kinetics and Mechanism of DGEBA Epoxy Resin with Phthalide-Containing Aromatic Diamine. *Thermochim. Acta* **2016**, *623*, 15−21.

(39) Achilias, D. S. Investigation of the Radical Polymerization Kinetics Using DSC and Mechanistic or Isoconversional Methods. *J. Therm. Anal. Calorim.* **2014**, *116* (3), 1379−1386.

(40) Wu, F.; Zhou, X.; Yu, X. Reaction Mechanism, Cure Behavior and Properties of a Multifunctional Epoxy Resin, TGDDM, with Latent Curing Agent Dicyandiamide. *RSC Adv.* **2018**, *8* (15), 8248−8258.

(41) Tarnacka, M.; Madejczyk, O.; Dulski, M.; Wikarek, M.; Pawlus, S.; Adrjanowicz, K.; Kaminski, K.; Paluch, M. Kinetics and Dynamics of the Curing System. High Pressure Studies. *Macromolecules* **2014**, *47* (13), 4288−4297.

(42) Maka, H.; Spychaj, T.; Pilawka, R. Epoxy Resin/Ionic Liquid Systems: The Influence of Imidazolium Cation Size and Anion Type on Reactivity and Thermomechanical Properties. *Ind. Eng. Chem. Res.* **2012**, *51* (14), 5197−5206.

(43) Neumeyer, T.; Staudigel, C.; Bonotto, G.; Altstaedt, V. Influence of an Imidazolium Salt on the Curing Behaviour of an Epoxy-Based Hot-Melt Prepreg System for Non-Structural Aircraft Applications. *CEAS Aeronaut. J.* **2015**, *6* (1), 31−37.

(44) Binks, F. C.; Cavalli, G.; Henningsen, M.; Howlin, B. J.; Hamerton, I. Examining the Effects of Storage on the Initiation Behaviour of Ionic Liquids towards the Cure of Epoxy Resins. *React. Funct. Polym.* **2018**, *133*, 9−20.

(45) Binks, F. C.; Cavalli, G.; Henningsen, M.; Howlin, B. J.; Hamerton, I. Investigating the Mechanism through Which Ionic Liquids Initiate the Polymerisation of Epoxy Resins. *Polymer* **2018**, *139* (1), 163−176.

(46) Guenther Soares, B.; Livi, S.; Duchet-Rumeau, J.; Gerard, J. F. Preparation of Epoxy/MCDEA Networks Modified with Ionic Liquids. *Polymer* **2012**, *53* (1), 60−66.

(47) Rahmathullah, M. A. M.; Jeyarajasingam, A.; Merritt, B.; VanLandingham, M.; McKnight, S. H.; Palmese, G. R. Room Temperature Ionic Liquids as Thermally Latent Initiators for Polymerization of Epoxy Resins. *Macromolecules* **2009**, *42* (9), 3219−3221.

(48) Heise, M. S.; Martin, G. C. Curing Mechanism and Thermal Properties of Epoxy—Imidazole Systems. *Macromolecules* **1989**, *22* (1), 99−104.

(49) Heise, M. S.; Martin, G. C. Analysis of the Cure Kinetics of Epoxy/Imidazole Resin Systems. *J. Appl. Polym. Sci.* **1990**, *39* (3), 721−738.

(50) Heise, M. S.; Martin, G. C.; Gotro, J. T. Characterization of Imidazole-Cured Epoxy-Phenol Resins. *J. Appl. Polym. Sci.* **1991**, *42* (6), 1557−1566.

(51) Ahn, Y. N.; Lee, S. H.; Lee, G. S.; Kim, H. Effect of Alkyl Branches on the Thermal Stability of Quaternary Ammonium Cations in Organic Electrolytes for Electrochemical Double Layer Capacitors. *Phys. Chem. Chem. Phys.* **2017**, *19* (30), 19959−19966.

(52) Partansky, A. M. A Study of Accelerators for Epoxy-Amine Condensation Reaction. *Adv. Chem. Ser.* **1970**, *92*, 29−47.

(53) Gaskamine 240 - Improvement of Curing Performance under Low Temperature Condition, Technical Service Report No. 03021H,

Ver. 1.0.; https://www.mgc.co.jp/eng/products/ac/pdf/TSR03021H-Ver1.0.pdf.

(54) Ochi, M.; Okazaki, M.; Shimbo, M. Mechanical Relaxation Mechanism of Epoxide Resins Cured With Aliphatic Diamines. *J. Polym. Sci., Polym. Phys. Ed.* **1982**, *20* (4), 689−699.

(55) Fournier, J.; Williams, G.; Duch, C.; Aldridge, G. A. Changes in Molecular Dynamics during Bulk Polymerization of an Epoxide-Amine System as Studied by Dielectric Relaxation Spectroscopy. *Macromolecules* **1996**, *29* (22), 7097−7107.

(56) Lorenzo, A. T.; Arnal, M. L.; Albuerne, J.; Müller, A. J. DSC Isothermal Polymer Crystallization Kinetics Measurements and the Use of the Avrami Equation to Fit the Data: Guidelines to Avoid Common Problems. *Polym. Test.* **2007**, *26* (2), 222−231.

(57) Parthun, M. G.; Johari, G. P. Dielectric Spectroscopy of a Polymerizing Liquid and the Evolution of Molecular Dynamics with Increase in the Number of Covalent Bonds. *J. Chem. Phys.* **1995**, *103* (1), 440−450.

(58) Mąka, H.; Spychaj, T.; Kowalczyk, K. Imidazolium and Deep Eutectic Ionic Liquids as Epoxy Resin Crosslinkers and Graphite Nanoplatelets Dispersants. *J. Appl. Polym. Sci.* **2014**, *131* (12), 40401.

(59) Carvalho, A. P. A.; Santos, D. F.; Soares, B. G. Epoxy/Imidazolium-based Ionic Liquid Systems: The Effect of the Hardener on the Curing Behavior, Thermal Stability, and Microwave Absorbing Properties. *J. Appl. Polym. Sci.* **2020**, *137* (5), 48326.

(60) Nguyen, T. K. L.; Livi, S.; Pruvost, S.; Soares, B. G.; Duchet-Rumeau, J. Ionic Liquids as Reactive Additives for the Preparation and Modification of Epoxy Networks. *J. Polym. Sci., Part A: Polym. Chem.* **2014**, *52* (24), 3463−3471.

(61) Swier, S.; Van Mele, B. Mechanistic Modeling of the Reaction Kinetics of Phenyl Glycidyl Ether (PGE) + Aniline Using Heat Flow and Heat Capacity Profiles from Modulated Temperature DSC. *Thermochim. Acta* **2004**, *411* (2), 149−169.

(62) Kong, M.; Liu, C.; Tang, B.; Xu, W.; Huang, Y.; Li, G. Improved Mechanical and Thermal Properties of Trifunctional Epoxy Resins through Controlling Molecular Networks by Ionic Liquids. *Ind. Eng. Chem. Res.* **2019**, *58* (19), 8080−8089.

(63) Wang, J.; Laborie, M. P. G.; Wolcott, M. P. Comparison of Model-Free Kinetic Methods for Modeling the Cure Kinetics of Commercial Phenol-Formaldehyde Resins. *Thermochim. Acta* **2005**, *439* (1−2), 68−73.

(64) Wang, J.; Laborie, M. P. G.; Wolcott, M. P. Comparison of Model-Fitting Kinetics for Predicting the Cure Behavior of Commercial Phenol-Formaldehyde Resins. *J. Appl. Polym. Sci.* **2007**, *105* (3), 1289−1296.

(65) Kamal, M. R.; Sourour, S. Kinetics and Thermal Characterization of Thermoset Cure. *Polym. Eng. Sci.* **1973**, *13* (1), 59−64.

(66) Corezzi, S.; Fioretto, D.; Santucci, G.; Kenny, J. M. Modeling Diffusion-Control in the Cure Kinetics of Epoxy-Amine Thermoset Resins: An Approach Based on Configurational Entropy. *Polymer* **2010**, *51* (24), 5833−5845.

(67) Zhang, C.; Binienda, W. K.; Zeng, L.; Ye, X.; Chen, S. Kinetic Study of the Novolac Resin Curing Process Using Model Fitting and Model-Free Methods. *Thermochim. Acta* **2011**, *523* (1−2), 63−69.

(68) Sourour, S.; Kamal, M. R. Differential Scanning Calorimetry of Epoxy Cure: Isothermal Cure Kinetics. *Thermochim. Acta* **1976**, *14* (1−2), 41−59.

(69) Avrami, M. Kinetics of Phase Change. I: General Theory. *J. Chem. Phys.* **1939**, *7* (12), 1103−1112.

(70) Avrami, M. Kinetics of Phase Change. II Transformation-Time Relations for Random Distribution of Nuclei. *J. Chem. Phys.* **1940**, *8* (2), 212−224.

(71) Avrami, M. Granulation, Phase Change, and Microstructure Kinetics of Phase Change. III. *J. Chem. Phys.* **1941**, *9* (2), 177−184.

(72) Weibing, X.; Pingsheng, H.; Dazhu, C. Cure Behavior of Epoxy Resin/Montmorillonite/Imidazole Nanocomposite by Dynamic Torsional Vibration Method. *Eur. Polym. J.* **2003**, *39* (3), 617−625.

(73) Lu, X. F.; Hay, J. N. Isothermal Crystallization Kinetics and Melting Behaviour of Poly(Ethylene Terephthalate). *Polymer* **2001**, *42* (23), 9423−9431.

(74) Kim, S.-W. W.; Lu, M.-G. G.; Shim, M.-J. J. The Isothermal Cure Kinetic of Epoxy/Amine System Analyzed by Phase Change Theory. *Polym. J.* **1998**, *30* (2), 90−94.

(75) Narine, S. S.; Humphrey, K. L.; Bouzidi, L. Modification of the Avrami Model for Application to the Kinetics of the Melt Crystallization of Lipids. *J. Am. Oil Chem. Soc.* **2006**, *83* (11), 913−921.

(76) Bianchi, O.; Oliveira, R. V. B.; Fiorio, R.; Martins, J. D. N.; Zattera, A. J.; Canto, L. B. Assessment of Avrami, Ozawa and Avrami-Ozawa Equations for Determination of EVA Crosslinking Kinetics from DSC Measurements. *Polym. Test.* **2008**, *27* (6), 722−729.

(77) Zhang, Z.; Xiao, C.; Dong, Z. Comparison of the Ozawa and Modified Avrami Models of Polymer Crystallization under Non-isothermal Conditions Using a Computer Simulation Method. *Thermochim. Acta* **2007**, *466* (1−2), 22−28.

(78) Binks, F. C.; Cavalli, G.; Henningsen, M.; Howlin, B. J.; Hamerton, I. Examining the Kinetics of the Thermal Polymerisation Behaviour of Epoxy Resins Initiated with a Series of 1-Ethyl-3-Methylimidazolium Based Ionic Liquids. *Thermochim. Acta* **2018**, *663*, 19−26.

(79) Maksym, P.; Tarnacka, M.; Bielas, R.; Hachuła, B.; Zajac, A.; Szpecht, A.; Smiglak, M.; Kaminski, K.; Paluch, M. Structure-Property Relationships of Tailored Imidazolium- and Pyrrolidinium-Based Poly(Ionic Liquid)s. Solid-like vs. Gel-like Systems. *Polymer* **2020**, *192*, 122262.

(80) Matsumoto, K.; Endo, T. Confinement of Ionic Liquid by Networked Polymers Based on Multifunctional Epoxy Resins. *Macromolecules* **2008**, *41* (19), 6981−6986.

(81) Chen, M.; White, B. T.; Kasprzak, C. R.; Long, T. E. Advances in Phosphonium-Based Ionic Liquids and Poly(Ionic Liquid)s as Conductive Materials. *Eur. Polym. J.* **2018**, *108*, 28−37.

(82) Wojnarowska, Z.; Knapik, J.; Díaz, M.; Ortiz, A.; Ortiz, I.; Paluch, M. Conductivity Mechanism in Polymerized Imidazolium-Based Protic Ionic Liquid [HSO3-BVIm][OTf]: Dielectric Relaxation Studies. *Macromolecules* **2014**, *47* (12), 4056−4065.

(83) Ganesan, V. Ion Transport in Polymeric Ionic Liquids: Recent Developments and Open Questions. *Mol. Syst. Des. Eng.* **2019**, *4* (2), 280−293.